.

Multichannel active noise control for spatially sparse noise fields

Jihui ZhangThushara D. Abhayapala, Prasanga N. Samarasinghe, and Wen ZhangShouda Jiang

Citation: The Journal of the Acoustical Society of America **140**, EL510 (2016); doi: 10.1121/1.4971878

View online: http://dx.doi.org/10.1121/1.4971878

View Table of Contents: http://asa.scitation.org/toc/jas/140/6

Published by the Acoustical Society of America

Multichannel active noise control for spatially sparse noise fields

Jihui Zhang[a)]
School of Electrical Engineering and Automation, Harbin Institute of Technology, Harbin Heilongjiang 150001, China
jihui.zhang@anu.edu.au

Thushara D. Abhayapala, Prasanga N. Samarasinghe, and Wen Zhang
Research School of Engineering, College of Engineering and Computer Science, The Australian National University, Canberra, ACT 2601, Australia
thushara.abhayapala@anu.edu.au, prasanga.samarasinghe@anu.edu.au, wen.zhang@anu.edu.au

Shouda Jiang
School of Electrical Engineering and Automation, Harbin Institute of Technology, Harbin Heilongjiang 150001, China
jsd@hit.edu.cn

Abstract: Multi-channel active noise control (ANC) is currently an attractive solution for the attenuation of low-frequency noise fields, in three-dimensional space. This paper develops a controller for the case when the noise source components are sparsely distributed in space. The anti-noise signals are designed as in conventional ANC to minimize the residual errors but with an additional term containing an ℓ_l norm regularization applied to the signal magnitude. This results in that only secondary sources close to the noise sources are required to be active for cancellation of sparse noise fields. Adaptive algorithms with low computational complexity and faster convergence speeds are proposed.

[SKL]
Date Received: August 30, 2016 **Date Accepted:** November 18, 2016

1. Introduction

Active noise control (ANC) developed based on the superposition principle employs secondary sources to generate anti-noise signals for cancellation of the primary noise.[1] To deal with noise in a three-dimensional (3D) space, such as in applications of noise cancellation in aircrafts and automobiles,[2] multi-channel (MC) ANC equipped with multiple sensors and multiple secondary sources is adopted.[3] As typical noise fields are often non-stationary, a common approach is to use adaptive filters to iteratively calculate the anti-noise signals that drive the secondary sources, in either feed-forward or feed-back control configurations. Feedback systems are of more interest as they avoid the need for separate reference sensors to measure the primary noise. The frequency domain MC ANC (Ref. 4) and its variation [such as Leaky ANC (Ref. 5)] are now widely used in practice for noise cancellation at error sensor positions and their close surroundings.[6]

When the noise source components are sparsely distributed in space (i.e., directional sparse noise field constructed by a few noise sources), such as industry noise field in an open area and directional sources in less reverberant rooms, an effective strategy is to use only the secondary sources that are close to the noise sources for noise cancellation. This means that many secondary source candidates in the MC ANC system can be inactive reducing the overall system complexity. The sparse feature is exploited by introducing an additional term to the cost function, which minimizes the residual error. This term contains an ℓ_1 norm penalty on the anti-noise signals. A similar solution is used in sound control and system identification applications exploiting sparsity.[7–9] For frequency domain MC ANC, the adaptive filters are designed in terms of complex vectors, so the ℓ_1 norm constraint should be applied accordingly.

In this paper, we develop two constrained MC ANC formulations to deal with spatially sparse distribution of noise sources. These algorithms are derived via

[a)]Author to whom correspondence should be addressed. Also at: Research School of Engineering, College of Engineering and Computer Science, The Australian National University, Canberra, ACT 2601, Australia.

combining two variants of the ℓ_1 norm of complex vectors into the conventional MC cost function. The complex ℓ_1 constrained multi-channel (Cℓ_1-MC) algorithm adds ℓ_1 norm constraint on the complex anti-noise signals, and the scalar ℓ_1 constrained multi-channel (Sℓ_1-MC) algorithm adds constraint on sum of the ℓ_1 norm to the real and imaginary part of the anti-noise signals. Simulations are conducted to evaluate the proposed two algorithms in comparison with the conventional MC and Leaky multi-channel (Leaky-MC) algorithm.

2. Problem formulation

Let the interested quiet zone be a two-dimensional (or height-invariant 3D) circular region with radius r. Assume that the noise sources are located outside of the interested region and have directional sparsity, as shown in Fig. 1. A single microphone array is placed on the boundary of the region to measure the residual signals and a single loudspeaker array is placed outside the control region to generate the anti-noise signals.[10]

The residual signal at any arbitrary observation point $\boldsymbol{x} \equiv \{\|\boldsymbol{x}\|, \phi_{\boldsymbol{x}}\}$ within the interested region is given by

$$e(\boldsymbol{x}, k) = \nu(\boldsymbol{x}, k) + s(\boldsymbol{x}, k), \tag{1}$$

where $k = 2\pi f/c$ is the wave number, f is the frequency, c is the speed of sound propagation, $\nu(\boldsymbol{x}, k)$ is the primary noise signal, and $\boldsymbol{s}(\boldsymbol{x}, k)$ is the secondary sound field generated by the loudspeakers. The sound field due to the secondary sources (loudspeaker array) is given by

$$s(\boldsymbol{x}, k) = \sum_{q=1}^{Q} d_q(k) G(\boldsymbol{x}|\boldsymbol{y}_q, k), \tag{2}$$

where $d_q(k)$ is the driving signal for the qth loudspeaker, and $G(\boldsymbol{x}|\boldsymbol{y}_q, k)$ denotes the acoustic transfer function (ATF) between the qth loudspeaker and the observation point $\boldsymbol{x}$. Let the microphones be positioned at $\boldsymbol{x}_p, p = 1, \ldots, P$ with respect to the origin O. Then the residual signal vector at the microphone array is given by

$$\boldsymbol{e} = \boldsymbol{v} + \boldsymbol{G}\boldsymbol{d}, \tag{3}$$

where $\boldsymbol{e} \triangleq [e(\boldsymbol{x}_1, k), \ldots, e(\boldsymbol{x}_P, k)]^T$, $\boldsymbol{v} \triangleq [\nu(\boldsymbol{x}_1, k), \ldots, \nu(\boldsymbol{x}_P, k)]^T$, $\boldsymbol{d} \triangleq [d_1(k), \ldots, d_Q(k)]^T$, $\boldsymbol{G}$ is a $P \times Q$ matrix with the (p, q) element given by $G(\boldsymbol{x}_p|\boldsymbol{y}_q, k)$. Superscript ^{T} denotes transpose of a vector or a matrix.

The objective is to design the anti-noise driving signals $\boldsymbol{d}$, using the minimum number of active secondary sources to generate secondary sound field and force the residual error signals $\boldsymbol{e}$ toward zero. In practical applications, the noise field is often unknown and time-varying. Therefore, we employ adaptive filters to iteratively update the weights.

3. Conventional adaptive ANC

3.1 MC ANC

The conventional MC approach minimizes the sum of the squares of the residual error signals with the cost function $\xi(n) = \sum_{p=1}^{P} |e_p(n)|^2 = \boldsymbol{e}^H(n)\boldsymbol{e}(n) = \|\boldsymbol{e}(n)\|_2^2$, where n is the iteration index of the adaptive algorithm, and $(\cdot)^H$ denotes the conjugate transpose.

By using the steepest descent algorithm, the adaptive filters are updated by

$$\boldsymbol{d}(n+1) = \boldsymbol{d}(n) - \frac{\mu}{2} \nabla \xi(n), \tag{4}$$

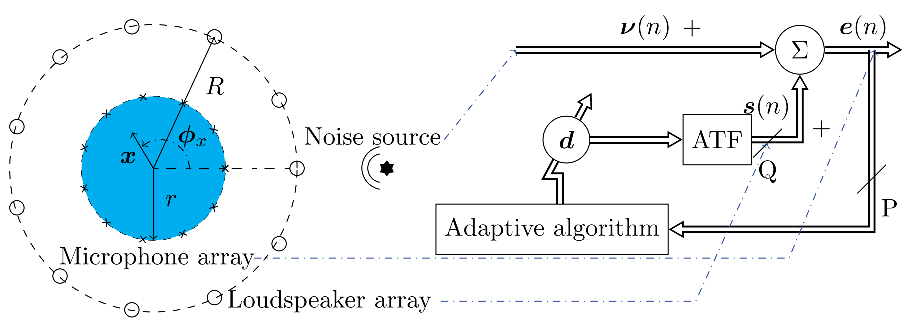

Fig. 1. (Color online) ANC setup with a circular region and the block diagram of the MC feedback ANC system.

where μ is the adaptation step size, $\nabla\xi(n) = 2\boldsymbol{G}^H\boldsymbol{e}(n)$ is the gradient of the cost function. The block diagram of the frequency domain MC feedback algorithm is shown in Fig. 1.

3.2 Leaky-MC ANC

The Leaky-MC algorithm introduces the output power constraints to the adaptive filter. By minimizing the sum of the squares of the residual error signals and the weighted sum of anti-noise signals,[11] the modified cost function is written as

$$\xi_{\text{Leaky}}(n) = \|\boldsymbol{e}(n)\|_2^2 + \rho\|\boldsymbol{d}(n)\|_2^2, \tag{5}$$

where ρ is the leakage factor greater than zero. It can be seen that $\nabla\xi_{\text{Leaky}}(n) = 2\boldsymbol{G}^H\boldsymbol{e}(n) + 2\rho\boldsymbol{d}(n)$. Hence the adaptive weights of the Leaky-MC algorithm are updated as

$$\boldsymbol{d}(n+1) = (1-\mu\rho)\boldsymbol{d}(n) - \mu\boldsymbol{G}^H\boldsymbol{e}(n). \tag{6}$$

4. Sparsity constrained adaptive ANC

In this section, we exploit the sparse nature of the noise sources to reduce the active loudspeaker numbers by introducing an additional constraint on the anti-noise signals into the cost function.

4.1 ℓ_0 norm constrained MC ANC

One method to enforce a reduction in the number of loudspeakers in MC ANC systems is by utilizing the compressed sensing techniques.[12] This can be done by selecting the amplitudes of the loudspeaker driving functions as the solution of the following constrained minimization problem:

$$\min_{\boldsymbol{d}(k)} \|\boldsymbol{e}(k)\|_2^2 + \delta(k)\|\boldsymbol{d}(k)\|_0, \tag{7}$$

where $\delta(k)$ is the sparsity level for each frequency bin, and $\|\boldsymbol{d}(k)\|_0$ represents a total number of non-zero elements in the anti-noise signal vector.

However, the problem in Eq. (7) is non-polynomial hard as it entails an exhaustive search. Therefore, the ℓ_0 norm is either approximated by a continuous function[13] or replaced by the ℓ_1 norm.[7] Because the ℓ_1 norm regularization is a convex problem, it can provide a sparse solution with less computational time. In this paper, we propose two regularization methods involving ℓ_1 norm in Secs. 4.2 and 4.3.

4.2 Complex ℓ_1 norm constrained MC ANC

We replace the ℓ_0 norm in Eq. (7) with the ℓ_1 norm on the complex vector

$$\min_{\boldsymbol{d}(k)} \underbrace{\|\boldsymbol{e}(k)\|_2^2 + \lambda(k)\|\boldsymbol{d}(k)\|_1}_{\xi_{\text{C}\ell_1\text{-MC}}}, \tag{8}$$

where $\|\boldsymbol{d}(k)\|_1$ is the sum of the magnitudes of the complex entries of the vector $\boldsymbol{d}(k)$, $\lambda(k)$ is a controllable parameter to determine the degree of sparse constraint for the adaptive coefficients.

In the frequency domain adaptive algorithm, combining the squared residual error signals with the ℓ_1 norm of the weight vector, the gradient of the cost function can be written as

$$\nabla\xi_{\text{C}\ell_1\text{-MC}}(n) = \underbrace{\nabla\|\boldsymbol{e}^H(n)\|_2^2}_{\nabla\xi_1(n)} + \underbrace{\nabla\lambda\|\boldsymbol{d}(n)\|_1}_{\nabla\xi_2(n)}, \tag{9}$$

where we dropped the frequency dependency and inserted the adaptive index n.

Theorem 1. *The gradient of the cost function*$\xi_{\text{C}\ell_1\text{-MC}}(n)$ *is given by*

$$\nabla\xi_{\text{C}\ell_1\text{-MC}}(n) = 2\boldsymbol{G}^H\boldsymbol{e}(n) + \lambda\exp(i\boldsymbol{\theta}(n)), \tag{10}$$

where $\boldsymbol{\theta}(n)$ *is the vector of phases of complex driving signals* $d_q(n)$, $q = 1, ..., Q$, *and* $\exp(\cdot)$ *denotes the exponential function.*

Proof. The term $\nabla\xi_1(n)$ of Eq. (9) is the same as that of the conventional MC algorithm, i.e., $\nabla\xi_1(n) = 2\boldsymbol{G}^H\boldsymbol{e}(n)$. From Eq. (9), we write[14] $\nabla\xi_2 = 2\lambda\partial(\|\boldsymbol{d}\|_1)/\partial\boldsymbol{d}^* = 2\lambda\partial(\sum_{q=1}^{Q}|d_q|)/\partial\boldsymbol{d}^*$, where the superscript * denotes the complex conjugate. Then

$$\frac{\partial\left(\sum_{q=1}^{Q}|d_q|\right)}{\partial \boldsymbol{d}^*} = \begin{bmatrix} \frac{\partial |d_1|}{\partial d_1^*} \\ \vdots \\ \frac{\partial |d_Q|}{\partial d_Q^*} \end{bmatrix} = \frac{1}{2}\begin{bmatrix} \frac{\partial |d_1|}{\partial \Re(d_1)} + i\frac{\partial |d_1|}{\partial \Im(d_1)} \\ \vdots \\ \frac{\partial |d_Q|}{\partial \Re(d_Q)} + i\frac{\partial |d_Q|}{\partial \Im(d_Q)} \end{bmatrix}. \tag{11}$$

Given the absolute value of a complex number $|d_q| = \sqrt{\Re(d_q)^2 + \Im(d_q)^2}$, where $\Re(\cdot)$ and $\Im(\cdot)$ denote the real and imaginary parts of the argument, we have

$$\frac{\partial |d_q|}{\partial \Re(d_q)} = \frac{\Re(d_q)}{\sqrt{\Re(d_q)^2 + \Im(d_q)^2}} = \cos\theta_q, \quad \frac{\partial |d_q|}{\partial \Im(d_q)} = \frac{\Im(d_q)}{\sqrt{\Re(d_q)^2 + \Im(d_q)^2}} = \sin\theta_q. \tag{12}$$

By substituting Eq. (12) into Eq. (11), $\nabla\xi_2$ can be simplified to $\lambda\exp(i\boldsymbol{\theta})$. This completes the proof. □

Following the steepest descent updating, the final update equation of the C ℓ_1-MC algorithm can be written as

$$\boldsymbol{d}(n+1) = \boldsymbol{d}(n) - \mu\boldsymbol{G}^H\boldsymbol{e}(n) - \frac{1}{2}\mu\lambda\exp(i\boldsymbol{\theta}(n)). \tag{13}$$

Compared to the conventional MC approach, the additional constraint $\frac{1}{2}\mu\lambda\exp(i\boldsymbol{\theta}(n))$ tends to shrink more entries in the anti-noise signals vector to zero. As evidenced in Sec. 5, this method speeds up the convergence in the spatially sparse noise fields.

4.3 Scalar ℓ_1 norm constrained MC ANC

In the second method, we replace the ℓ_0 norm in Eq. (7) with the sum of the ℓ_1 norm on the real and imaginary part of the anti-noise signals. The new cost function becomes

$$\xi_{S\ell_1\text{-MC}}(n) = \|\boldsymbol{e}^H(n)\|_2^2 + \lambda(\|\Re(\boldsymbol{d}(n))\|_1 + \|\Im(\boldsymbol{d}(n))\|_1). \tag{14}$$

Instead of forcing the complex weight entries toward zero directly, we force the real and imaginary parts of the complex entries toward zero at the same rate.

Theorem 2. *The gradient of the cost function* $\xi_{S\ell_1\text{-MC}}(n)$ *is given by*

$$\nabla\xi_{S\ell_1\text{-MC}}(n) = \underbrace{\nabla\|\boldsymbol{e}^H(n)\|_2^2}_{\nabla\xi_1(n)} + \underbrace{\nabla\lambda(\|\Re(\boldsymbol{d}(n))\|_1 + \|\Im(\boldsymbol{d}(n))\|_1)}_{\nabla\xi_2'(n)} \tag{15}$$

$$= 2\boldsymbol{G}^H\boldsymbol{e}(n) + \lambda(\operatorname{sgn}(\Re(\boldsymbol{d}(n))) + i\operatorname{sgn}(\Im(\boldsymbol{d}(n)))), \tag{16}$$

where $\operatorname{sgn}(\cdot)$ *is a component-wise function which is defined as*

$$\operatorname{sgn}(d) = \begin{cases} d/|d| & d \neq 0 \\ 0 & d = 0. \end{cases}$$

Proof.

$$\nabla\xi_2' = 2\lambda\left(\frac{\partial(\|\Re(\boldsymbol{d})\|_1)}{\partial\boldsymbol{d}^*} + \frac{\partial(\|\Im(\boldsymbol{d})\|_1)}{\partial\boldsymbol{d}^*}\right). \tag{17}$$

The complex partial differentiation based on $\boldsymbol{d}^*$ can be separated by[15]

$$\frac{\partial\|\Re(\boldsymbol{d})\|_1}{\partial\boldsymbol{d}^*} = \frac{1}{2}\left(\frac{\partial\|\Re(\boldsymbol{d})\|_1}{\partial\Re(\boldsymbol{d})} + i\frac{\partial\|\Re(\boldsymbol{d})\|_1}{\partial\Im(\boldsymbol{d})}\right) \text{ and } \frac{\partial\|\Im(\boldsymbol{d})\|_1}{\partial\boldsymbol{d}^*} = \frac{1}{2}\left(\frac{\partial\|\Im(\boldsymbol{d})\|_1}{\partial\Re(\boldsymbol{d})} + i\frac{\partial\|\Im(\boldsymbol{d})\|_1}{\partial\Im(\boldsymbol{d})}\right). \tag{18}$$

Each item in Eq. (18) can be given by

$$\frac{\partial\|\Re(\boldsymbol{d})\|_1}{\partial\Re(\boldsymbol{d})} = \operatorname{sgn}(\Re(\boldsymbol{d})), \quad \frac{\partial\|\Re(\boldsymbol{d})\|_1}{\partial\Im(\boldsymbol{d})} = \frac{\partial\|\Im(\boldsymbol{d})\|_1}{\partial\Re(\boldsymbol{d})} = 0 \text{ and } \frac{\partial\|\Im(\boldsymbol{d})\|_1}{\partial\Im(\boldsymbol{d})} = \operatorname{sgn}(\Im(\boldsymbol{d})). \tag{19}$$

By substituting Eqs. (18) and (19) into Eq. (17), we obtain the second term of Eq. (16). Also note from Theorem 1 $\nabla\xi_1(n) = 2\boldsymbol{G}^H\boldsymbol{e}(n)$ which is the first term of Eq. (16). □

Thus, the scalar ℓ_1 norm constrained adaptive algorithm (Sℓ_1-MC) can be written as

$$\boldsymbol{d}(n+1) = \boldsymbol{d}(n) - \mu \boldsymbol{G}^H \boldsymbol{e}(n) - \frac{1}{2}\mu\lambda(\mathrm{sgn}(\Re(\boldsymbol{d}(n))) + i\,\mathrm{sgn}(\Im(\boldsymbol{d}(n)))). \tag{20}$$

Compared to Eq. (13), in Eq. (20) the exponential function of a complex vector is replaced by the sign function of two real vectors, which can save the computational complexity in each iteration. It is a significant advantage in the real time implementations.

5. Simulation results

We compare the proposed algorithms (Cℓ_1-MC and Sℓ_1-MC) with the MC algorithm[4] and the Leaky-MC algorithm[11] in a free-field environment. Let the desired quiet zone be a circular region of radius of 1 m. The ANC system consists of 11 microphones placed equi-angularly on the boundary of the region and 11 loudspeakers placed on a circle of $R = 2$ m. A point noise source is placed at 0° at a radius of 2.5 m. A signal-to-noise ratio of 40 dB white Gaussian noise is added at each microphone recording. To evaluate the noise reduction (NR) performance inside the region (NR$_{\text{in}}$), sound pressure ($\boldsymbol{e}_{\text{in}}$) at $M = 1296$ uniformly placed points inside the regions are examined. We define $\mathrm{NR}_{\text{in}}(n)$ as follows:

$$\mathrm{NR}_{\text{in}}(n) = 10\log_{10}\frac{\|\boldsymbol{e}_{\text{in}}(n)\|_2^2/M}{\|\boldsymbol{e}_{\text{in}}(0)\|_2^2/M}, \tag{21}$$

where $\boldsymbol{e}_{\text{in}}(n)$ denotes the residual signals on the points inside the region at the nth iteration, and $\boldsymbol{e}_{\text{in}}(0)$ represents the primary noise field in the region. The sparsity parameter

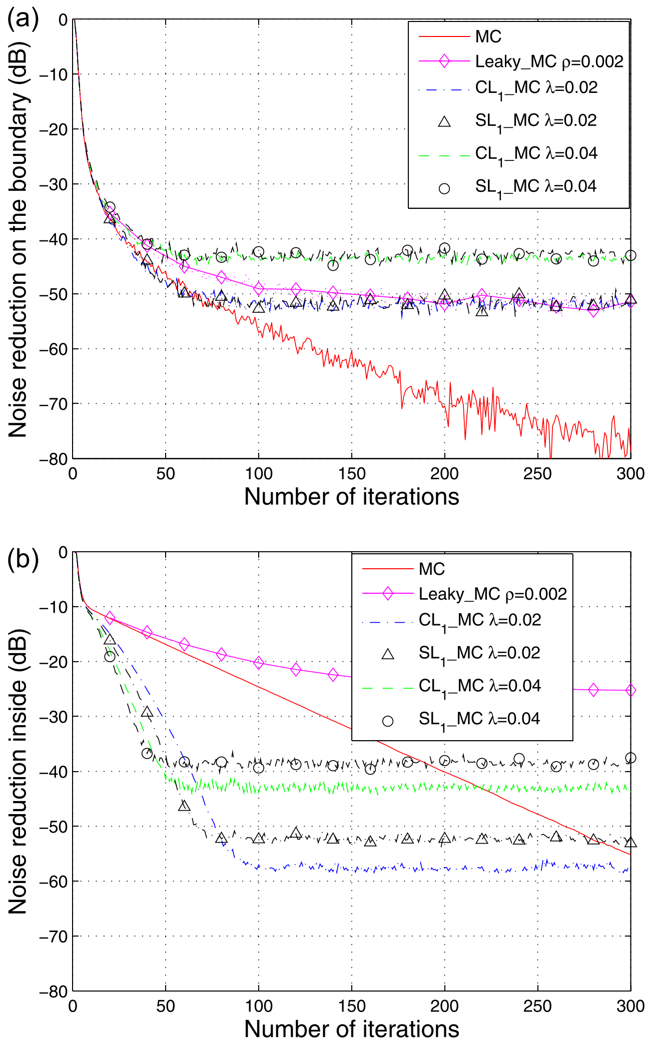

Fig. 2. (Color online) Comparison of the convergence speed and NR level using different ANC algorithms: (a) NR on the boundary and (b) NR inside the region.

$\lambda(k)$ can be searched over the set $[0, \|G(k)^H \mathbf{v}(k)\|_\infty)$, and the selection depends on a trade-off between the active loudspeaker number and the NR level in the steady state. As the primary noise field is often unknown, we can estimate the noise level using the microphone recordings and obtain the searching range. During the adaptive process, if significant changes happen to the microphone recordings, $\lambda(k)$ needs to be reset to fit the varying noise field.

First, we investigate the narrowband performance of different algorithms. The frequency of the noise field is 200 Hz. The initial value of $\boldsymbol{d}$ is $\boldsymbol{d}(0) = [0, 0, ..., 0]^T$, and hence $\boldsymbol{\theta}(0) = [0, 0, ..., 0]^T$. Figure 2 shows the convergence performance and the NR level for each iteration. Compared with MC, adding the ℓ_1 constraint will dramatically increase the convergence speed, especially for NR inside the region, but adding the power constraint (Leaky-MC) can only slightly increase the speed. For NR performance, adding the constraint to the anti-noise signals (Cℓ_1-MC, Sℓ_1-MC, and Leaky-MC) will decrease NR in steady state. From the comparison of Figs. 2(a) and 2(b), we can see that for the Leaky-MC algorithm, after convergence, the NR performance inside the region is much worse than NR on the boundary. While for the same λ, both Cℓ_1-MC and Sℓ_1-MC can achieve a similar NR level in steady state on the microphone points and inside the region. Since our motivation is to cancel the noise over the entire region, the proposed Cℓ_1-MC and Sℓ_1-MC algorithms have considerable improvement than the conventional MC and Leaky-MC algorithms.

Figure 3 demonstrates the performance in terms of the energy of anti-noise signals and active loudspeaker numbers. Here we define the jth loudspeaker is active when $\|\boldsymbol{d}_j\| > 2\%\|\boldsymbol{d}_{\max}\|$. From Fig. 3(a), compared to MC, the constrained MC

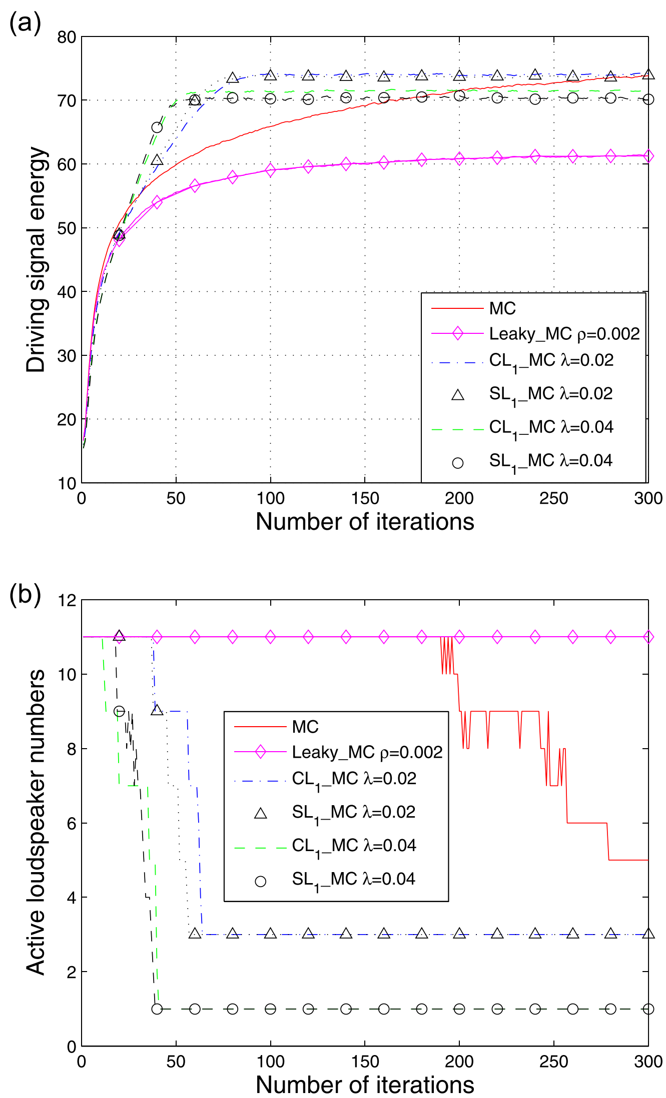

Fig. 3. (Color online) Comparison of the anti-noise signals using different ANC algorithms: (a) loudspeaker driving signal energy for each iteration and (b) active loudspeaker numbers for each iteration.

Table 1. Broadband performance using different ANC algorithms.

Frequency (Hz)	NR boundary (dB)			NR inside (dB)			Active speaker numbers		
	MC	$C\ell_1$-MC	$S\ell_1$-MC	MC	$C\ell_1$-MC	$S\ell_1$-MC	MC	$C\ell_1$-MC	$S\ell_1$-MC
50	−53.04	−49.50	−48.83	−69.47	−62.28	−58.67	11	4	5
100	−48.30	−38.62	−38.76	−65.94	−49.39	−48.25	9	3	3
150	−46.88	−43.58	−40.49	−38.43	−49.61	−49.69	9	3	3
200	−50.89	−43.25	−40.41	−20.84	−41.04	−35.84	11	1	2
250	−81.20	−41.81	−38.57	−66.44	−41.22	−35.73	7	1	1
300	−49.85	−41.98	−40.05	−22.22	−38.98	−38.98	9	1	1

algorithms can reduce the total energy of the anti-noise signals, which can avoid the overloading of the secondary sources. For the Leaky-MC algorithm, all the loudspeaker candidates are active in steady state, as shown in Fig. 3(b). Whereas both $C\ell_1$-MC and $S\ell_1$-MC can reduce the active loudspeaker numbers, over the conventional algorithms. After convergence, the loudspeakers which are far away from the noise source are non-active. A larger value of λ will force more loudspeakers non-active. When $\lambda = 0.04$, both $C\ell_1$-MC and $S\ell_1$-MC can reduce the active loudspeaker numbers from 11 to 1, which corresponds to the case that only the loudspeaker candidate located at 0° is active in the steady state. When the primary sound field is constructed by multiple primary sources, for example, two primary sources in different locations, the results are found to be similar to that containing a single primary source.

Table 1 shows the broadband performance for different algorithms after 50 iterations. The frequency range of the noise field is [50, 300] Hz. For the MC algorithm, the NR is not converged, thus the NRs inside the region are not stable over the frequency range. For the proposed algorithms, by selecting a proper parameter value for each frequency, 40 to 50 dB NR can be achieved on the boundary and inside the region. Compared to the MC algorithm, both $C\ell_1$-MC and $S\ell_1$-MC can reduce the active loudspeaker numbers. From the comparison of the proposed algorithms, we can see that $C\ell_1$-MC has a slightly better broadband performance than $S\ell_1$-MC, but $S\ell_1$-MC can achieve a significant NR with less computational complexity.

Acknowledgment

This work is supported by Australian Research Council (ARC) Discovery Projects funding scheme (project no. DP140103412). The work of J.Z. was sponsored by the China Scholarship Council with the Australian National University.

References and links

[1]C. C. Fuller, S. J. Elliott, and P. A. Nelson, *Active Control of Vibration* (Academic, San Diego, CA, 1996).
[2]J. I. Mohammad, S. J. Elliott, and A. Mackay, "The performance of active control of random noise in cars," J. Acoust. Soc. Am. **123**, 1838–1841 (2008).
[3]Y. Kajikawa, W.-S. Gan, and S. M. Kuo, "Recent advances on active noise control: Open issues and innovative applications," APSIPA Trans. Signal Inf. Process. **1**, 21 (2012).
[4]T. Kosaka, S. J. Elliott, and C. C. Boucher, "A novel frequency domain filtered-x LMS algorithm for active noise reduction," in *Proceedings of the IEEE ICASSP*, Vol. 1, Munich, Germany (1997), pp. 403–406.
[5]S. J. Elliott, I. Stothers, and P. A. Nelson, "A multiple error LMS algorithm and its application to the active control of sound and vibration," IEEE Trans. Acoustics Speech Signal Process. **35**, 1423–1434 (1987).
[6]J. Lorente, M. Ferrer, M. De Diego, and A. González, "GPU implementation of multichannel adaptive algorithms for local active noise control," IEEE/ACM Trans. Audio Speech Lang. Process. **22**, 1624–1635 (2014).
[7]G. Lilis, D. Angelosante, and G. Giannakis, "Sound field reproduction using the lasso," IEEE Trans. Audio Speech Lang. Process. **18**, 1902–1912 (2010).
[8]Y. Chen, Y. Gu, and A. Hero, "Sparse LMS for system identification," in *Proceedings of the IEEE ICASSP*, Taipei, Taiwan (2009), pp. 3125–3128.
[9]K. Shi and X. Ma, "Transform domain LMS algorithms for sparse system identification," in *Proceedings of the IEEE ICASSP*, Dallas, TX (2010), pp. 3714–3717.
[10]J. Zhang, W. Zhang, and T. D. Abhayapala, "Noise cancellation over spatial regions using adaptive wave domain processing," in *Proceedings of the IEEE WASPAA*, New York (2015), pp. 1–5.
[11]S. J. Elliott, *Signal Processing for Active Control* (Academic Press, New York, 2000), pp. 132–149.
[12]E. J. Candes and M. B. Wakin, "An introduction to compressive sampling," IEEE Signal Process. Mag. **25**, 21–30 (2008).
[13]J. Weston, A. Elisseeff, B. Schölkopf, and M. Tipping, "Use of the zero norm with linear models and kernel methods," J. Machine Learn. Res. **3**, 1439–1461 (2003).
[14]S. Haykin, *Adaptive Filter Theory* (Prentice Hall, Englewood Cliffs, NJ, 2001), pp. 794–798.
[15]D. Sarason, *Complex Function Theory* (American Mathematical Society, Providence, 2007).